

UNITED STATES PATENT AND TRADEMARK OFFICE

UNITED STATES DEPARTMENT OF COMMERCE
United States Patent and Trademark Office
Address: COMMISSIONER FOR PATENTS
P.O. Box 1450
Alexandria, Virginia 22313-1450
www.uspto.gov

TJW

APPLICATION NO.	FILING DATE	FIRST NAMED INVENTOR	ATTORNEY DOCKET NO.	CONFIRMATION NO.
10/544,266	01/10/2006	Dong-Kyun Seo	4647-AIPCUS	1339
51493	7590	09/25/2006	EXAMINER	
GREG MARTINEZ 1522 E. SOUTHERN AVE. # 1002 TEMPE, AZ 85282			VANOY, TIMOTHY C	
		ART UNIT	PAPER NUMBER	1754

DATE MAILED: 09/25/2006

Please find below and/or attached an Office communication concerning this application or proceeding.

BEST AVAILABLE COPY

Office Action Summary	Application No.	Applicant(s)	
	10/544,266	SEO ET AL.	
	Examiner Timothy C. Vanoy	Art Unit 1754	

-- The MAILING DATE of this communication appears on the cover sheet with the correspondence address --

Period for Reply

A SHORTENED STATUTORY PERIOD FOR REPLY IS SET TO EXPIRE 3 MONTH(S) OR THIRTY (30) DAYS, WHICHEVER IS LONGER, FROM THE MAILING DATE OF THIS COMMUNICATION.

- Extensions of time may be available under the provisions of 37 CFR 1.136(a). In no event, however, may a reply be timely filed after SIX (6) MONTHS from the mailing date of this communication.
- If NO period for reply is specified above, the maximum statutory period will apply and will expire SIX (6) MONTHS from the mailing date of this communication.
- Failure to reply within the set or extended period for reply will, by statute, cause the application to become ABANDONED (35 U.S.C. § 133). Any reply received by the Office later than three months after the mailing date of this communication, even if timely filed, may reduce any earned patent term adjustment. See 37 CFR 1.704(b).

Status

- 1) Responsive to communication(s) filed on 01 August 2005.
- 2a) This action is FINAL. 2b) This action is non-final.
- 3) Since this application is in condition for allowance except for formal matters, prosecution as to the merits is closed in accordance with the practice under *Ex parte Quayle*, 1935 C.D. 11, 453 O.G. 213.

Disposition of Claims

- 4) Claim(s) 35-54 is/are pending in the application.
 - 4a) Of the above claim(s) _____ is/are withdrawn from consideration.
- 5) Claim(s) _____ is/are allowed.
- 6) Claim(s) 35-54 is/are rejected.
- 7) Claim(s) _____ is/are objected to.
- 8) Claim(s) _____ are subject to restriction and/or election requirement.

Application Papers

- 9) The specification is objected to by the Examiner.
- 10) The drawing(s) filed on 01 August 2005 is/are: a) accepted or b) objected to by the Examiner.

Applicant may not request that any objection to the drawing(s) be held in abeyance. See 37 CFR 1.85(a).

Replacement drawing sheet(s) including the correction is required if the drawing(s) is objected to. See 37 CFR 1.121(d).
- 11) The oath or declaration is objected to by the Examiner. Note the attached Office Action or form PTO-152.

Priority under 35 U.S.C. § 119

- 12) Acknowledgment is made of a claim for foreign priority under 35 U.S.C. § 119(a)-(d) or (f).
 - a) All b) Some * c) None of:
 1. Certified copies of the priority documents have been received.
 2. Certified copies of the priority documents have been received in Application No. _____.
 3. Copies of the certified copies of the priority documents have been received in this National Stage application from the International Bureau (PCT Rule 17.2(a)).
- * See the attached detailed Office action for a list of the certified copies not received.

Attachment(s)

- 1) Notice of References Cited (PTO-892)
- 2) Notice of Draftsperson's Patent Drawing Review (PTO-948)
- 3) Information Disclosure Statement(s) (PTO/SB/08)
Paper No(s)/Mail Date _____
- 4) Interview Summary (PTO-413)
Paper No(s)/Mail Date _____
- 5) Notice of Informal Patent Application
- 6) Other: _____

DETAILED ACTION

Claim Rejections - 35 USC § 112

The following is a quotation of the second paragraph of 35 U.S.C. 112:

The specification shall conclude with one or more claims particularly pointing out and distinctly claiming the subject matter which the applicant regards as his invention.

Claims 38-40 and 46 are rejected under 35 U.S.C. 112, second paragraph, as being indefinite for failing to particularly point out and distinctly claim the subject matter which applicant regards as the invention.

- a) Claims 38-40 are vague and indefinite because it is not clear exactly what the relationship is between the provision of the second and third materials and the amount of heat. What happens to the provision of the second and third materials if the amount of heat is decreased? What happens to the provision of the second and third materials if the amount of heat is increased?
- b) Claim 46 is vague and indefinite because it is not clear how the nanocrystals "operate" as a nanowire. This claim does not provide and details concerning this "operation".

Claim Rejections - 35 USC § 102

The following is a quotation of the appropriate paragraphs of 35 U.S.C. 102 that form the basis for the rejections under this section made in this Office action:

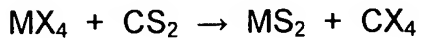
A person shall be entitled to a patent unless –

- (b) the invention was patented or described in a printed publication in this or a foreign country or in public use or on sale in this country, more than one year prior to the date of application for patent in the United States.

Art Unit: 1754

Claims 35-40 are rejected under 35 U.S.C. 102(b) as being anticipated by U. S. Patent 4,208,394 to Chianelli.

U. S. Patent 4,208,394 in col. 2 Ins. 18-37 describes a reaction between a halide of at least one Group Ivb or Vb transition metal and carbon disulfide to form a transition metal sulfide and carbon tetrahalide, according to:



where M is at least one Group Ivb or Vb transition metal and X is at least one halide. Col. 2 Ins. 59-61 in U. S. Patent 4,208,394 sets forth that the reaction may be in the liquid phase.

Claims 35-40 are rejected under 35 U.S.C. 102(b) as being anticipated by U. S. Patent 4,678,584 to Elfline.

U. S. Patent 4,678,584 in col. 3 Ins. 29-39 describes what appears to be a liquid phase reaction between an aqueous solution of sodium hydroxide and carbon disulfide to form sodium trithiocarbonate, according to:



Claims 41-48 are rejected under 35 U.S.C. 102(b) as being anticipated by U. S. 6,303,097 B1 to Kinsman et al.

Claim 1 in U. S. Patent 6,303,097 B1 sets forth a method for making metal sulfide, comprising:

reacting an elemental carbon (i. e. the applicants' "third material") with gaseous hydrogen sulfide (i. e. the applicants' "second material") to produce gaseous carbon disulfide (i. e. the applicants' "fourth material") at a temperature of 900-1,500 °C (i. e. the applicants' "first amount of heat"), and

passing the gaseous carbon disulfide into a second reaction zone which contains metal oxide (i. e. the applicants' "first material") so as to result in a reaction between the carbon disulfide and the metal oxide to produce metal sulfide (i. e. the applicants' "fifth material") at a temperature of 500-1,500 °C (i. e. the applicants' "second amount of heat").

Claims 49-54 are rejected under 35 U.S.C. 102(b) as being anticipated by U. S. Patent 5,958,281 to Takada et al.

Example 1 in U. S. Patent 5,958,281 describes a method for making $0.01\text{Li}_3\text{PO}-0.63\text{Li}_2\text{S}-0.36\text{SiS}_2$ glass from various lithium sulfides and silicon sulfides, comprising:

- providing lithium sulfide (i. e. the applicants' "first material");
- providing a bath of molten sulfur (i. e. the applicants' "chalcogen material");
- providing silicon powder (i. e. the applicants' "second material which is reactive with the chalcogen material");
- reacting the molten sulfur and silicon powder together to form silicon sulfide (i. e. the applicants' "third material"), and

Art Unit: 1754

reacting the lithium sulfide and silicon sulfide together to form the lithium ion-conductive solid electrolyte which formed the oxysulfide glass represented by the formula: 0.01Li₃PO-0.63Li₂S-0.36SiS₂ (i. e. the applicants' "fourth material").

Claims 41-54 rejected under 35 U.S.C. 102(b) as being anticipated by the English abstract of CN 1251348.

The English abstract of CN 1251348 describes what appears to be the same method for manufacturing what appears to be the same metal sulfides (i. e. "semiconductor materials") by reacting a metal salt; a non-metal element (such as S, Se, Te. . . etc.) and a boron hydride in the presence of an organic solvent to produce the semiconductor materials.

The following references are made of record:

U. S. Patent 5,279,801 disclosing the production of binary rare earth/sulfur or transition metal/sulfur compounds from a rare earth oxide (or transition metal oxide) and carbon disulfide (please see the abstract);

U. S. Patent 4,557,914 disclosing a process for producing substances that are optically transparent to infra-red rays via a reaction between chalcogen hydride and a metal halide;

U. S. Patent 4,542,009 disclosing the use of mixed metal sulfides as battery electrodes (please see col. 3 lns. 17-31), and

Art Unit: 1754

U. S. Patent 4,374,037 disclosing a method for making divalent europium activated calcium sulfide phosphors.

The following references from the applicants' Search Report are made of record:

U. S. Patent 4,778,539 disclosing a process for producing a PbMo₆S₈ type compound superconductor;

U. S. Patent 3,770,422 disclosing a process for purifying Eu and Tb and forming refractory compounds therefrom;

U. S. Patent 3,009,977 disclosing a thermoelectric material; and
the article titled "Bulk Synthesis of Inorganic Fullerene-like MS₂ (M = Mo, W) from the Respective Trioxides and the Reaction Mechanism" by Y. Feldman et al. disclosing the synthesis of inorganic fullerene-MS₂.

Any inquiry concerning this communication or earlier communications from the examiner should be directed to Timothy C. Vanoy whose telephone number is 571-272-8158. The examiner can normally be reached on Mon-Fri 8-4:30.

If attempts to reach the examiner by telephone are unsuccessful, the examiner's supervisor, Stanley Silverman, can be reached on 571-272-1358. The fax phone number for the organization where this application or proceeding is assigned is 571-273-8300.

Art Unit: 1754

Information regarding the status of an application may be obtained from the Patent Application Information Retrieval (PAIR) system. Status information for published applications may be obtained from either Private PAIR or Public PAIR. Status information for unpublished applications is available through Private PAIR only. For more information about the PAIR system, see <http://pair-direct.uspto.gov>. Should you have questions on access to the Private PAIR system, contact the Electronic Business Center (EBC) at 866-217-9197 (toll-free). If you would like assistance from a USPTO Customer Service Representative or access to the automated information system, call 800-786-9199 (IN USA OR CANADA) or 571-272-1000.

Timothy C. Vanoy
Timothy C Vanoy
Primary Examiner
Art Unit 1754

tv

Notice of References Cited		Application/Control No.	Applicant(s)/Patent Under Reexamination SEO ET AL.	
		Examiner Timothy C. Vanoy	Art Unit 1754	Page 1 of 1

U.S. PATENT DOCUMENTS

*		Document Number Country Code-Number-Kind Code	Date MM-YYYY	Name	Classification
*	A	US-6,303,097 B1	10-2001	Kinsman et al.	423/561.1
*	B	US-5,958,281	09-1999	Takada et al.	429/305
*	C	US-5,279,801	01-1994	Colombet et al.	423/21.1
*	D	US-4,778,539	10-1988	Kubo et al.	423/511
*	E	US-4,678,584	07-1987	Elfline, Geraldine S.	210/719
*	F	US-4,557,914	12-1985	Modone, Eros	423/303
*	G	US-4,542,009	09-1985	Palmer, David N.	148/239
*	H	US-4,374,037	02-1983	Takahashi, Tatsuo	252/301.4S
*	I	US-4,208,394	06-1980	Chianelli, Russell R.	423/561.1
*	J	US-3,770,422	11-1973	Darnell, Alfred J.	75/370
*	K	US-3,009,977	11-1961	HOUSTON MAURICE D	136/204
L	US-				
M	US-				

FOREIGN PATENT DOCUMENTS

*		Document Number Country Code-Number-Kind Code	Date MM-YYYY	Country	Name	Classification
	N					
	O					
	P					
	Q					
	R					
	S					
	T					

NON-PATENT DOCUMENTS

*		Include as applicable: Author, Title Date, Publisher, Edition or Volume, Pertinent Pages)
	U	The English abstract of CN 1251348 A published on 04/26/2000.
	V	Feldman, Y. et al. "Bulk Synthesis of Inorganic Fullerine-like MS2 (M = Mo, W) from the Respective Trioxides and the Reaction Mechanism" Journal of the American Chemical Society, Vol. 118, No. 23 (1996), pgs. 5362-5367.
	W	
	X	

*A copy of this reference is not being furnished with this Office action. (See MPEP § 707.05(a).)
Dates in MM-YYYY format are publication dates. Classifications may be US or foreign.

AN 2000:864660 CAPLUS
 DN 134:6605
 ED Entered STN: 12 Dec 2000
 TI Preparation of nanometer compounds of sulfur family or phosphorous family
 IN Qian, Yitai; Wang, Wenzhong
 PA China Science and Technology Univ., Peop. Rep. China
 SO Faming Zhuanli Shenqing Gongkai Shuomingshu, 5 pp.
 CODEN: CNXXEV

DT Patent

LA Chinese

IC ICM C01B017-20

ICS C01B025-00

CC 49-5 (Industrial Inorganic Chemicals)

FAN.CNT 1

	PATENT NO.	KIND	DATE	APPLICATION NO.	DATE
PI	<u>CN 1251348</u>	A	20000426	<u>CN 1998-119471</u>	19981015
	<u>CN 1086177</u>	B	20020612		
PRAI	<u>CN 1998-119471</u>			19981015	

CLASS

	PATENT NO.	CLASS	PATENT FAMILY CLASSIFICATION CODES
	<u>CN 1251348</u>	ICM	C01B017-20
		ICS	C01B025-00
		IPCI	C01B0017-20 [ICM,7]; C01B0017-00 [ICM,7,C*]; C01B0025-00 [ICS,7]
		IPCR	C01B0017-00 [I,C*]; C01B0017-20 [I,A]; C01B0025-00 [I,A]; C01B0025-00 [I,C*]

AB The process comprises reacting metal salt (formulated by MXn, M = Cu, Ag, Zn, Cd, Hg, Fe, Co, Ni, Ge, Sn, Pb, Al, Ga, In, As, Sb or Bi; X = F-, Cl-, Br-, I-, NO3- or SO42-) with non-metal element and boron hydrides in the presence of org. solvent, filtering, washing, and drying. The non-metal element is selected from S, Se, Te, P, As or Sb; the boron hydride is selected from LiBH4, NaBH4 or KBH4; and the solvent is selected from benzene, toluene, 1,2-ethanediamine, polyamine, pyridine, CS2, and THF. The process is simple, low in cost, and suitable for substantial prodn. of semiconductor materials.

ST chalcogenide compd manuf boron hydride reaction; phosphorous compd manuf boron hydride reaction

IT Nanoparticles

(manuf. of nanometer compds. of sulfur family or phosphorous family)

IT Semiconductor materials

(manuf. of nanometer compds. of sulfur family or phosphorous family for)

IT 7447-39-4, Copper dichloride, reactions 7646-85-7, Zinc chloride, reactions 7718-54-9, Nickel chloride, reactions 7723-14-0, Phosphorus, reactions 7758-95-4, Lead chloride 7761-88-8, Silver nitrate, reactions 7772-99-8, Tin dichloride, reactions 7782-49-2, Selenium, reactions 7784-34-1, Arsenic trichloride 7787-60-2, Bismuth chloride 10025-82-8, Indium chloride 10025-91-9, Antimony chloride SbCl3 10108-64-2, Cadmium chloride

RL: RCT (Reactant); TEM (Technical or engineered material use); RACT (Reactant or reagent); USES (Uses)

(in manuf. of nanometer compds. of sulfur family or phosphorous family)

IT 1302-09-6P, Silver selenide 1303-36-2P, Arsenic selenide As2Se3 1306-24-7P, Cadmium selenide, preparation 1314-05-2P, Nickel selenide 1315-05-5P, Antimony selenide 1315-06-6P, Tin selenide SnSe 1315-09-9P, Zinc selenide 12035-64-2P, Nickel phosphide Ni2P 12068-69-8P, Bismuth selenide 12069-00-0P, Lead selenide 20405-64-5P, Copper selenide Cu2Se 22398-80-7P, Indium phosphide, preparation

IT RL: IMF (Industrial manufacture); PREP (Preparation)
(manuf. of nanometer compds. of sulfur family or phosphorous family)
13762-51-1, Potassium borohydride 16940-66-2, Sodium borohydride
16949-15-8, Lithium borohydride
RL: RCT (Reactant); TEM (Technical or engineered material use); RACT
(Reactant or reagent); USES (Uses)
(manuf. of nanometer compds. of sulfur family or phosphorous family)

[First Hit](#) [Previous Doc](#) [Next Doc](#) [Go to Doc#](#)

End of Result Set

[Generate Collection](#) | [Print](#)

L1: Entry 1 of 1

File: DWPI

Jun 12, 2002

DERWENT-ACC-NO: 2000-424146

DERWENT-WEEK: 200523

COPYRIGHT 2006 DERWENT INFORMATION LTD

TITLE: Method for preparing nanometer material - of compound of sulfur family and phosphorus family

INVENTOR: QIAN, Y ; WANG, W

PATENT-ASSIGNEE:

ASSIGNEE	CODE
UNIV CHINESE SCI & TECHNOLOGY	UYCHN

PRIORITY-DATA: 1998CN-0119471 (October 15, 1998)

[Search Selected](#) | [Search ALL](#) | [Clear](#)

PATENT-FAMILY:

PUB-NO	PUB-DATE	LANGUAGE	PAGES	MAIN-IPC
<input type="checkbox"/> CN 1086177 C	June 12, 2002		000	C01B017/20
<input type="checkbox"/> CN 1251348 A	April 26, 2000		000	C01B017/20

APPLICATION-DATA:

PUB-NO	APPL-DATE	APPL-NO	DESCRIPTOR
CN 1086177C	October 15, 1998	1998CN-0119471	
CN 1251348A	October 15, 1998	1998CN-0119471	

INT-CL (IPC): C01B 17/20; C01B 25/00

ABSTRACTED-PUB-NO: CN 1251348A

BASIC-ABSTRACT:

The preparation method of chalcogenide or phosphorus family compound nanometer material is characterized by that mixing the metal salt, chalcogen or phosphorus family non-metallic elementary substance and hydroborates metered according to its chemical reaction equation in organic solvent, completely reacting, filtering, washing and drying to obtain the invented product.

ADVANTAGE - The invention is implemented at room-temperature, is simple in operation and easy to implement, its raw material is cheap and easily available, it can save energy source, reduce cost, and is safe in operation and applicable to large-scale production of chalcogen and phosphorus family semiconductive material.

CHOSEN-DRAWING: Dwg.0

TITLE-TERMS: METHOD PREPARATION MATERIAL COMPOUND SULPHUR FAMILY PHOSPHORUS FAMILY

DERWENT-CLASS: E36 L03

CPI-CODES: E31-K04; L03-D01;

SECONDARY-ACC-NO:

CPI Secondary Accession Numbers: C2000-128629

[Previous Doc](#)

[Next Doc](#)

[Go to Doc#](#)

Bulk Synthesis of Inorganic Fullerene-like MS_2 ($\text{M} = \text{Mo, W}$) from the Respective Trioxides and the Reaction Mechanism

Y. Feldman,[†] G. L. Frey,[†] M. Homyonfer,[†] V. Lyakhovitskaya,[†] L. Margulis,^{†,‡}
H. Cohen,[‡] G. Hodes,^{*,†} J. L. Hutchison,[§] and R. Tenne^{*,†}

Contribution from the Department of Materials and Interfaces, Weizmann Institute, Rehovot 76100, Israel, Department of Chemical Services, Weizmann Institute, Rehovot 76100, Israel, and Department of Materials, University of Oxford, Parks Road, Oxford OX1 3PH, U.K.

Received January 23, 1996[¶]

Abstract: Recently, milligram quantities of MoS_2 fullerene-like nanotubes and negative curvature polyhedra (generically called *inorganic fullerene-like material, IF*), were reproducibly obtained by a gas phase reaction from an oxide precursor (Feldman, Y.; Wasserman, E.; Srolovitz, D. J.; Tenne, R. *Science* 1995, 267, 222. Srolovitz, D. J.; Safran, S. A.; Homyonfer, M.; Tenne, R. *Phys. Rev. Lett.* 1995, 74, 1778). The present work focuses on the mechanism of the synthesis of IF- MS_2 ($\text{M} = \text{W, Mo}$). The IF material is obtained from oxide particles smaller than ca. $0.2\ \mu\text{m}$, while larger oxide particles result in 2H- MS_2 platelets. The key step in the reaction mechanism is the formation of a closed layer of MS_2 , which isolates the nanoparticle from its surroundings and prevents its fusion into larger particles. Subsequently, the oxide core of the nanoparticle is progressively converted into a sulfide nanoparticle with an empty core (IF). Taking advantage of this process, we report here a routine for the fabrication of macroscopic quantities of a pure IF- WS_2 phase with a very high yield. As anticipated, the size distribution of the IF material is determined by the size distribution of the oxide precursor. The present synthesis paves the way for a systematic study of these materials which are promising candidates for, e.g., solid lubrication.

Introduction

Notwithstanding the efforts to develop synthetic routes for the mass production of carbon fullerenes, nested fullerenes ("buckyonions"), nanotubes, etc., the generic technique for the synthesis of such phases remains arc-discharge^{3,4} and subsequent extraction from the soot. A similar process is also used for the synthesis of BN or $\text{B}_x\text{C}_y\text{N}_z$ nanotubes,^{5,6} metallocarbohedrenes (Met-Cars),⁷ endohedral fullerenes,⁸ and nanotubes.⁹ Obviously, this method is neither very easy to control nor amenable to an easy scale-up. The ensuing purification processes are tedious and time consuming, which influences the cost of the final product. Key steps in the growth mechanism of these products were elucidated,^{10,11} but the detailed mechanism of the reaction is still a matter of controversy. Therefore, the size distribution

of nanotubes and nested fullerenes cannot be adequately controlled and is relatively wide. For both species, the innermost layer serves as a template for the growth of the top layers, which usually grow outward,^{11–13} possibly in an accretion (snail-like) growth mode.¹⁴ The synthesis of inorganic MX_2 ($\text{M} = \text{W, Mo}; \text{X} = \text{S, Se}$) nested fullerene-like structures and nanotubes has been described recently.¹⁵ This study demonstrated that the propensity to form polyhedral structure is not unique to carbon, but is likely to be commonplace among nanoparticles of 2-D layered compounds.¹⁶ Subsequently, a gas phase synthesis of molybdenum trioxide precursor was used to obtain a few milligrams of IF- MoS_2 (IF = inorganic fullerene-like material).^{1,2} In contrast to the synthesis of carbon-nested fullerenes, the present process lends itself for an easy scale-up using low-cost feedstocks, and therefore relatively inexpensive products could be foreseen.

In this paper we present a model for the growth mechanism of the IF- MS_2 phase from an oxide precursor. Although the syntheses of the IF phases of MoS_2 and WS_2 differ in some important details, the salient features are common to both products. A schematic representation of the growth mode of an IF particle is depicted in Figure 1. Within the first few seconds of the reaction, the top surface of the oxide nanoparticle reacts with H_2S gas and a completely closed monomolecular MS_2 layer or two are formed. Similar behavior of oxide nanoparticles in H_2S atmosphere has been inadvertently ob-

- [†] Department of Materials and Interfaces, Weizmann Institute.
- [‡] Department of Chemical Services, Weizmann Institute.
- [§] University of Oxford.
- [¶] Abstract published in *Advance ACS Abstracts*, May 15, 1996.
- (1) Feldman, Y.; Wasserman, E.; Srolovitz, D. J.; Tenne, R. *Science* 1995, 267, 222.
- (2) Srolovitz, D. J.; Safran, S. A.; Homyonfer, M.; Tenne, R. *Phys. Rev. Lett.* 1995, 74, 1778.
- (3) Krätschmer, W. A.; Lamb, L. D.; Fostiropoulos, K.; Huffman, D. R. *Nature* 1990, 347, 354.
- (4) Ebbesen, T. W.; Ajayan, P. M. *Nature* 1992, 358, 220.
- (5) Stephane, O.; Ajayan, P. M.; Colliex, C.; Redlich, Ph.; Lambert, J. M.; Bernier, P.; Lefin, P. *Science* 1994, 266, 1683.
- (6) Weng-Sieh, Z.; Cherrey, K.; Chopra, N. G.; Blase, X.; Miyamoto, Y.; Rubio, A.; Cohen, M. L.; Louie, S. G.; Zettl, A.; Gronsky, R. *Phys. Rev. B* 1994, 51, 11229.
- (7) Cartier, S. F.; Chen, Z. Y.; Walder, G. J.; Sleppy, C. R.; Castleman, A. W. *Science* 1995, 260, 195.
- (8) (a) Chai, Y.; Guo, T.; Jin, C.; Haufner, R. E.; Chibante, L. P. F.; Fure, J.; Wang, L.; Alford, J. M.; Smalley, R. E. *J. Phys. Chem.* 1991, 95, 7564. (b) Takata, M.; Umeda, B.; Nishibori, E.; Sakata, M.; Saito, Y.; Ohno, M.; Shinohara, H. *Nature* 1995, 377, 46.
- (9) (a) Ruoff, R. S.; Lorent, D. C.; Chan, B.; Malhorta, R.; Subramoney, S. *Science* 1993, 259, 346. (b) Tomita, M.; Saito, Y.; Hayashi, T. *Jpn. J. Appl. Phys. I* 1993, 32, L280. (c) Seraphin, S.; Zhou, D.; Jiao, J.; Withers, J. C.; Lotfy, R. *Nature* 1993, 362, 503. (d) Yosida, Y. *Appl. Phys. Lett.* 1993, 62, 3447.
- (10) Jarrold, M. J.; et al. *J. Phys. Chem.* 1994, 98, 1810.

- (11) (a) Iijima, S. *Mater. Sci. Eng.* 1993, B19, 172. (b) Iijima, S.; Ajayan, P. M.; Ichihashi, T. *Phys. Rev. Lett.* 1992, 69, 3100.
- (12) Ugarte, D. *Nature* 1992, 359, 707.
- (13) (a) Ugarte, D. *Chem. Phys. Lett.* 1992, 198, 596. (b) Ugarte, D. Z. *Phys. D: At., Mol. Clusters* 1993, 26, 150. (c) Ugarte, D. *Europhys. Lett.* 1993, 22, 45.
- (14) Kroto, H. W. *Science* 1988, 242, 1139.
- (15) (a) Tenne, R.; Margulis, L.; Genut, M.; Hodes, G. *Nature* 1992, 360, 444. (b) Margulis, L.; Salitra, G.; Tenne, R.; Talianker, M. *Nature* 1993, 365, 113. (c) Hershfinkel, M.; Gheber, L. A.; Volterra, V.; Hutchison, J. L.; Margulis, L.; Tenne, R. *J. Am. Chem. Soc.* 1994, 116, 1914.
- (16) Chopra, N. G.; Luyken, R. J.; Cherrey, K.; Crespi, V. H.; Cohen, M. L.; Louie, S. G.; Zettl, A. *Science* 1995, 269, 966.

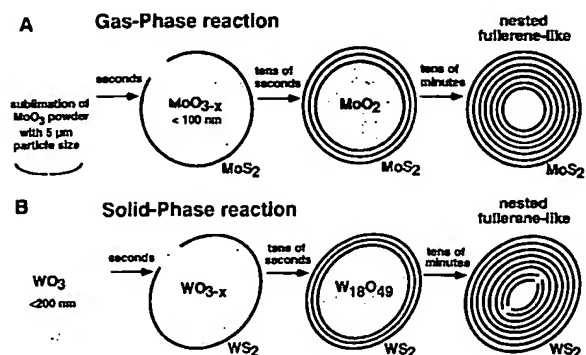


Figure 1. Schematic representation of the growth model of the inorganic fullerene-like phase of MoS_2 (A) and WS_2 (B) nested polyhedra from oxide nanoparticles.

served before.¹⁷ The inert surface–sulfide layer prohibits fusion of nanoparticles into macroscopic entities, which would lead to the formation of the 2H- MS_2 phase. Fast hydrogen diffusion into the nanoparticle leads to a complete reduction of the oxide core into MoO_2 or $\text{W}_{18}\text{O}_{49}$, within a minute or two.¹⁸ Subsequently, the oxide core is progressively converted into the respective sulfide (IF) through a slow diffusion-controlled reaction, which ends after ca. 30 min. Consequently, the size of the IF particle is determined by the size of the incipient oxide nanoparticle.

Experimental Section

Molybdenum oxide is volatile under reducing conditions above 700 °C, and hence a gas phase reaction was adopted for the synthesis of IF- MoS_2 .¹⁹ A detailed account of the gas phase reaction for the synthesis of IF- MoS_2 has been reported previously¹² and will be repeated only briefly here. Typically a portion of 30 mg of MoO_3 powder (>99% pure) is heated (>800 °C) and is slowly reduced to MoO_{3-x} by a stream of forming gas (typically 5% H_2 /95% N_2).²⁰ The suboxide sublimes and effuses out of a nozzle where it crosses a stream of H_2S gas mixed with a forming gas. It takes 3–5 min. for the entire load of MoO_3 to sublime. The reaction products are collected on a quartz substrate, which is positioned 3 cm away from the crossing point of the two gas streams and is maintained at the same temperature (>800 °C). The collected nanoparticles are progressively converted into nested IF polyhedra within ca. 30 min of firing time. The average size of the oxide nanoparticle and the ensuing IF- MoS_2 increases with temperature. It was found that above 900 °C, platelets with 2H- MoS_2 structure abound, and become the sole product above 950 °C.

Since WO_3 is not volatile at these temperatures, the solid (WO_3)–gas ($\text{H}_2\text{S} + \text{H}_2$) reaction was preferred, in this case.^{15a} The starting material for the synthesis of IF- WS_2 is a WO_3 powder (>99% pure), with particle sizes smaller than ca. 150 nm. To avoid agglomeration and fusion of the heated nanoparticles, the powder was carefully dispersed on the entire floor of the reactor boat, resulting in a complete exposure of the nanoparticle surface to the reacting gas. 2H- WS_2 platelets were predominantly obtained under the following experimental conditions: packing of the powder was too compact; oxide particles with sizes above 0.2 μm were used; the reaction temperature exceeded 900 °C.

Complementary information on the reaction mechanism was obtained by using a combination of the following techniques: transmission electron microscopy (TEM), electron diffraction (ED), X-ray powder

diffraction (XRD), X-ray photoelectron spectroscopy (XPS), and optical absorption measurements.

Results and Discussion

Figure 2 shows a series of TEM images demonstrating the progression of the conversion of MoO_2 particles into IF- MoS_2 (A–D). Since, the sublimation of the MoO_3 powder is not instantaneous, the extent of oxide to sulfide conversion of the nanoparticles is not uniform, particularly at the early stages of the process. Therefore, the number of MoS_2 layers varies from point to point on the quartz collector. Parts A–C of Figure 2 exhibit a series of stages in the conversion of a typical sample, which was retracted from the oven after 5 min. Figure 2A shows a number of MoO_2 particles covered by two to three closed layers of MoS_2 . Particles covered with four layers of MoS_2 , which were collected at another location of the quartz slide, are displayed in Figure 2B. Figure 2C shows a particle with at least six closed layers of MoS_2 . Electron diffraction (inset) confirmed that the inner core of the IF consists of MoO_2 .²¹ Most remarkably, a growth front of eight layers, which is seldom observed, is advancing into the oxide core on the upper-right side of the IF. The intermediate zone between the crystalline MoO_2 core and the advancing front of IF- MoS_2 appears structureless and is likely to consist of a disordered molybdenum oxysulfide.²² An assortment of completely converted IF- MoS_2 particles is shown in Figure 2D, and is typically obtained after 30 min of reaction time at 850 °C. The growth mechanism can be regarded in terms of a substitution model which is the opposite of the accretion model proposed previously for carbon fullerenes.¹⁴ The size of the MoO_{3-x} nanoparticles, which sublime from the MoO_3 source and are deposited on the quartz collector, increases with the temperature from 10 nm at 820 °C to 100 nm and above at 870 °C.¹ Therefore, the size of an IF particle is fully determined by the size of the incipient oxide nanoparticle which serves as its precursor. It is noticed that, while the particles exhibit a more spherical-like morphology in the beginning of the sulfidization process (Figure 2A,B), they show faceted morphology, with cusps and well-defined angles at the end of the process (Figure 2D). Moreover, the outer layers which are obtained in the initial stages of the sulfidization process remain mostly unchanged at the end of the process (Figure 2D), while the innermost layers with a smaller diameter exhibit much more faceted morphology. Edge dislocations are being formed and observed between the two morphologies. A continuum model has recently been used to calculate the shape of nested fullerenes. This model predicted a phase transformation from structures with spherical shape into faceted ones as the thickness (number of layers) of the particles increases beyond a critical value or the radius of curvature decreases beyond a certain critical value.² This qualitative agreement between theory and experiment indicates that continuum models can provide useful guidelines for IF synthesis.

In the case of IF- WS_2 , the precursor is solid WO_3 , and hence the size of the oxide nanoparticles (Figure 2E,G) determines the size of the IF particles (Figure 2F,H). In contrast to the molybdenum case, the H_2S gas reacts uniformly with all oxide particles in the powder, and hence the number of sulfide layers is essentially the same for all intermediate IF- WS_2 /oxide composite nanoparticles.

Figure 3 presents the XRD spectra of a WO_3 powder acquired during different stages of the annealing process. The XRD pattern of the precursor coincides with that of WO_3 (Figure 3A).

(17) Sanders, J. V. *J. Electron Microsc. Tech.* 1986, 3, 67.

(18) *Transition Metal Oxides*, Kung, H. H., Ed.; Amsterdam–Oxford–New York–Tokyo, 1989, Vol. 45, p 93.

(19) Although the main route for the synthesis of IF- MoS_2 was through the gas phase reaction, a solid–gas reaction was used as well. The details of the reaction were very similar to those of IF- WS_2 , but the yield was appreciably smaller due to sublimation of some of the oxide powder.

(20) The forming gas is necessary in order to reduce the more stable oxide and divert the reaction path to the sulfide products.

(21) Schmidt, E.; Weill, F.; Meunier, G.; Levasseur, A. *Thin Solid Films* 1995, 260, 21.

(22) Schmidt, E.; Sourisseau, C.; Meunier, G.; Levasseur, A. *Thin Solid Films* 1994, 245, 34.

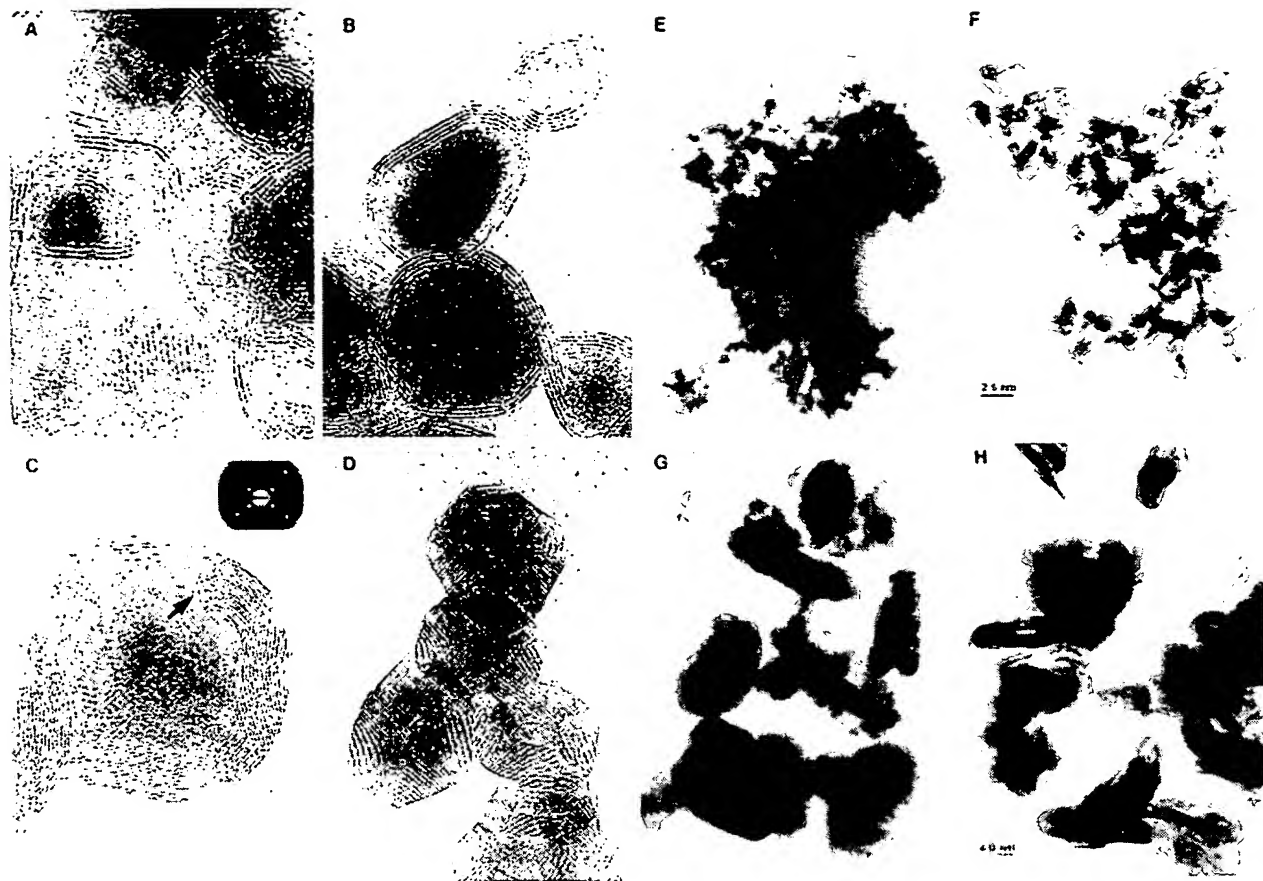


Figure 2. TEM micrographs showing the gradual transformation of molybdenum oxide nanoparticles into IF-MoS₂ (A–D) nested polyhedra. The electron diffraction pattern inset of (C) is consistent with (111) of MoO₂. (E) shows a typical assortment of tungsten oxide particles with <10 nm diameter which are transformed into IF-WS₂ particles of a similar size (Figure 2F). (G) and (H) show a similar transformation for tungsten oxide particles with a diameter in the range of 50–100 nm. Note that both oxide and IF phases contain very asymmetric particles. The interlayer spacing of 0.62 nm is clearly visible in (A)–(D).

After 2 min of annealing, a small WS₂ peak was observed (Figure 3B). Astonishingly, the entire nanoparticle core has been reduced to W₁₈O₄₉ at this early stage of the process. This fact can be understood assuming that hydrogen and water diffuse appreciably faster than sulfur diffuses to form sulfide. Figure 3C shows the state of the sample after 8 min of annealing, while Figure 3D displays the XRD patterns of the sample after 15 min of annealing time. The fully converted sample (120 min) is shown in Figure 3E. The shift of the (0002) peak of the IF-WS₂ phase (Figure 3D) indicates a lattice expansion of ca. 2% between two adjacent WS₂ slabs along the *c*-axis, which is attributed to the strain in the bent layers.¹ Furthermore, since the number of atoms in the layer increases with its radius, the layers cannot be fully commensurate. This discrepancy can be partially alleviated by lattice expansion along the *c*-axis. A similar study has been carried out for the conversion of MoO₂ into IF-MoS₂, the results being essentially the same as those shown in Figure 3.

Optical absorption spectra at different temperatures were measured for a sample consisting of IF-MoS₂ (shell)/MoO₂ (core) particles at different annealing times, including a pure IF-MoS₂ film (Figure 4A). A reference 2H-MoS₂ crystal was measured as well. Comparison of the spectra of IF-MoS₂ to that of the (2H) bulk phase at the same temperature reveals a red shift in the excitonic absorption of the former. The A, B, and C excitons appear at 667, 616.3, and 525 nm, respectively, in the IF phase at 175 K, while their energies in the 2H phase

are 654.3, 593.5, and 490 nm.^{23,24} After 3 min of annealing time of the oxide, the A and B excitons of the sulfide are already noticeable. The C exciton partially overlaps with the dominant absorption of MoO₂ at 500 nm.²⁵ The intensity of the oxide absorption decreased, while the exciton absorption increased with annealing time. After 90 min of annealing time, the exciton absorption peaks of the sulfide increased by a factor of 2.5 compared with the 3 min annealed sample. The oxide absorption disappeared completely. The transformation of WO_{3-x} into IF-WS₂ (Figure 4B) was followed by using stirred alcoholic suspensions at room temperature. The oxide absorption peak of the composite oxide/sulfide (6 min annealing time) could be easily resolved in the difference spectrum and is substantially red shifted, compared to the literature value.²⁵ Remarkably, IF-MS₂ powder consisting of particles smaller than 10 nm formed a stable alcoholic colloid exhibiting a strong blue shift of the excitonic absorption, which could be possibly assigned to a quantum size effect.²⁴

Being a surface sensitive technique, XPS could be ideally suited for investigating the sulfide/oxide superstructure. Accordingly, a few milligrams of IF-WS₂ powder, synthesized by the solid–gas reaction, was pressed onto an indium plate, which provided the support and electrical contact for the powder. A

(23) Wilson, J. A.; Yoffe, A. D. *Adv. Phys.* 1968, 18, 193.

(24) Frey, G. L.; Homyonfer, M.; Feldman, Y.; Tenne, R. To be published.

(25) Porter, V. R.; White, W. B.; Roy, R. *J. Solid State Chem.* 1969, 1, 359.

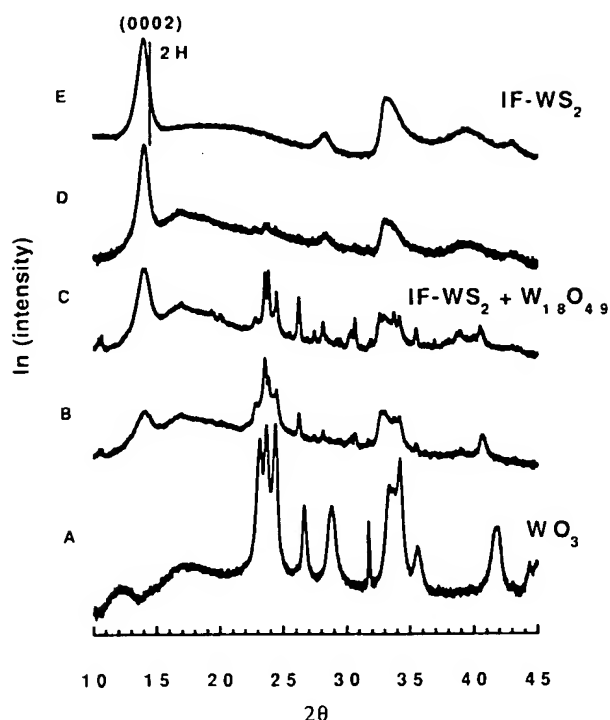


Figure 3. Transformation of WO_3 nanoparticles into IF- WS_2 followed by X-ray powder diffraction: (A) WO_3 precursor; (B) the same powder after 2 min of annealing; (C) after 8 min of annealing; (D) 15 min of annealing. Annealing conditions: 850 °C; rates of gas flow, forming gas, 130 cm^3/min ; H_2S , 2 cm^3/min .

sequence of four samples consisting of composite nanoparticles of IF- WS_2 (shell)/tungsten oxide (core) at different annealing times at 850 °C were investigated: sample 1, 2 min; 2, 6 min, 3, 15 min; 4, 2 h. In addition, reference WS_2 crystal, WO_3 powder, and a clean indium specimen were measured. The fraction of oxide particle converted into sulfide was determined in two independent ways, which gave similar results. The concentration of the two compounds was determined first from the analysis of the total concentrations of the various elements, and second from the tungsten 4f–5p spectral region which was deconvoluted into sulfide ($4f_{7/2}$, 32.6; $4f_{5/2}$, 34.75; $5p_{3/2}$, 38.3 eV) and oxide (shifted to higher energies by 3.0 eV). Shirley background subtraction was used for spectral analysis.²⁶ While the indium contribution to the total signal was less than 1%, carbon made up to 18% of the total material. Yet, by comparing the molybdenum and sulfur line shapes with those of pure 2H- MoS_2 , it was concluded that the carbon was not incorporated in the fullerene-like nanoparticles. The source of carbon contamination is likely to originate from adsorbed organic molecules having a mean thickness of 4–7 Å. Such an adsorbant signal does not seriously influence the analysis of its support, the fullerene-like material. Removal of the carbon contamination by ion sputtering was harmful to the IF structures and is not presented. Additional confirmation of that point came from local (TEM) electron energy loss measurements, which proved (due to its low sensitivity to surface contamination) that each nanoparticle consisted exclusively of Mo and S.

The spectra of 2H- WS_2 crystal and oxide powder, with line broadening permitted, were used as model line shapes for the deconvolution. The total error in this calculation was estimated at 1%. The high reliability of the deconvolution procedure was reaffirmed by using different pass energies. The results,

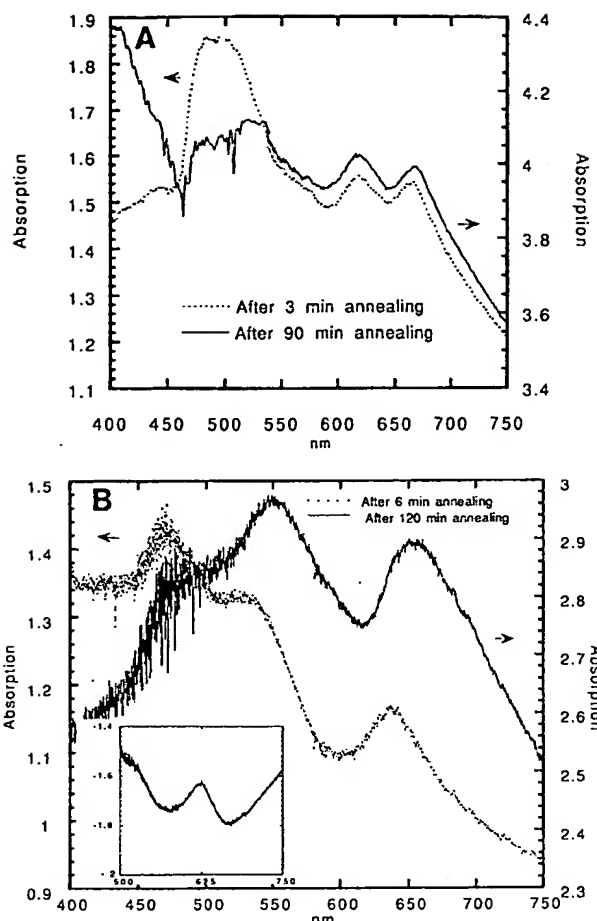


Figure 4. Optical absorption measurements of (A) a composite IF- MoS_2/MoO_2 sample obtained through the gas phase reaction and accrued on a quartz substrate after 3 min of annealing (dashed line) and after prolonged (90 min) annealing (solid line) and (B) a composite IF- WS_2/VO_{3-x} sample after 6 min of annealing (dashed line) and after 120 min of annealing (solid line). The inset shows the difference spectra (oxide absorption peak). Annealing conditions are as in Figure 3.

Table 1. Conversion of Tungsten Oxide into IF- WS_2 , Obtained from the Deconvolution of the W (4f) Peaks in a Series of XPS Spectra^a

annealing time (min)	I_{ox} (%)	I_{sul} (%)	d/λ	k
2	38	62	0.6	2
6	11	89	1.5	5
15	1.5	98.5	3.3	11
120	<0.5	>99.5		

^a Monochromatized Al K α ($h\nu = 1486.6$ eV) was used for the excitation. A monochromatized beam (0.7 eV resolution) and a base pressure of 10^{-9} Torr were used.

expressed as I_{sul} and I_{ox} , are summarized in Table 1. The relative intensities I_{sul}/I_{ox} can be converted into sulfide shell thickness (d) or number of dichalcogenide layers (k) by considering a model type polyhedron, for which the shell and core intensities are calculated face by face:

$$I_{sul}/I_{ox} = \sum W_n I_{n,sul} / \sum W_n I_{n,ox} \quad (1)$$

where W_n is the projection of the face area on the plane normal to the electron take-off direction (that is, parallel to the substrate plane). For simplicity we choose a regular polyhedron for the

(26) *Practical Surface Analysis*, 2nd ed.; Briggs, D., Seah, M. P., Eds.; John Wiley & Sons: New York, 1990, Vol. 1, p 233.

Table 2. Kinetics of the Reduction of WO_3 Nanoparticles into Suboxides and its Conversion into IF- WS_2 Studied by XRD for Samples Prepared under Different Experimental Conditions

gas atmosphere; flow rate (cm^3/min)	av size of oxide particles (μm)	temp ($^\circ\text{C}$)	reactn time (h)	product of reactn (XRD)	av particle size (μm) (TEM)
$\text{H}_2\text{S}; 4.5 + \text{H}_2(5\%)/\text{N}_2; 100$	3–5	500	3	WO_3	not changed
		640	1	$\text{WS}_2 + \text{W}_{20}\text{O}_{58}$	0.1–3
		820	1	$\text{WS}_2 + \text{W}_{20}\text{O}_{58} + \text{W}_{18}\text{O}_{49}$	
		870	2	2H- $\text{WS}_2 + \text{W}_{18}\text{O}_{49}$	2–10
		970	1	2H- $\text{WS}_2 + \text{WO}_2 + \text{W}_{18}\text{O}_{49}$	
	~0.1	150	18	WO_3	not changed
		300	9	WS_2/WO_3	
		400	4	$\text{WS}_2/\text{W}_{20}\text{O}_{58}$	
		700	0.3	IF- $\text{WS}_2/\text{W}_{20}\text{O}_{58}$	
		820	0.3	IF- $\text{WS}_2/\text{W}_{18}\text{O}_{49}$	
$\text{H}_2(5\%)/\text{N}_2; 100$	~0.1	820	2	IF- WS_2	
		870	2	IF- $\text{WS}_2 + 2\text{H-WS}_2 + \text{W}_{18}\text{O}_{49}$	2–10
		970	1	2H- $\text{WS}_2 + \text{W}_{18}\text{O}_{49} + \text{WO}_2$	
		560	2	WO_3	not changed
		570	1.5	$\text{W}_{20}\text{O}_{58}$	
	3–5	600	1	$\text{W}_{20}\text{O}_{58} + \text{W} + \text{W}_{18}\text{O}_{49}$	0.06–0.1
		650	1.5	$\text{WO}_2 + \text{W}$	0.03–0.1
		770	0.2	$\text{W}_{18}\text{O}_{49}$	0.1–1
		820	0.3	$\text{W}_{18}\text{O}_{49}$	1–2
		970	0.3	$\text{WO}_2 + \text{W}$	1–6
$\text{H}_2(1\%)/\text{N}_2; 100$	~0.1	630	1	WO_3	not changed
		650	1.5	$\text{WO}_3 + \text{WO}_2$	0.1–3
		750	0.2	$\text{W}_{20}\text{O}_{58}$	
		970	0.3	WO_2	1–6
		600	1.5	WO_3	not changed

analysis. The two I_n terms in eq 1 are given by²⁷

$$I_{n,\text{ sul}} = \int_0^{d/\cos\theta_n} dz I_{0(\text{sul})} \exp(-z/\lambda \cos \theta_n) + \int_{D_n + d/\cos\theta_n}^{D_n + 2d/\cos\theta_n} dz I_{0(\text{sul})} \exp(-z/\lambda \cos \theta_n) \\ I_{n,\text{ ox}} = \int_{d/\cos\theta_n}^{D_n + d/\cos\theta_n} dz I_{0(\text{ox})} \exp(-z/\lambda \cos \theta_n) \quad (2)$$

The two terms in $I_{n,\text{ sul}}$ stand for the contributions from the top and bottom shells of the n th segment (slope). I_0 is a factor proportional to the partial density of tungsten in the compound: $I_{0(\text{sul})} = I_0/3$; $I_{0(\text{ox})} = I_0/3.7$. D_n is the thickness of the oxide under the face of segment n . λ is the escape depth of the photoelectrons.

The calculated values for d/λ and k , which are given in Table 1, were obtained for a polyhedron having only six different slopes (segments): $\theta_n = 15^\circ n$, $n = 0, \dots, N - 1$. The number of slopes, $N = 6$, is a representative value. In fact the numerical result becomes only weakly dependent on N for $N > 3$. A similar model for spherical particles ($N \rightarrow \infty$) was recently published.²⁸ The value of λ was taken as $\sim 2 \text{ nm}^{29}$ and that of the interlayer distance as $\sim 0.62 \text{ nm}^{23}$. The results of this analysis are in good agreement with the TEM observations; the main error stems from the variation in the number of MS_2 layers in the various nested polyhedra. XPS analysis of the MoO_2 into IF- MoS_2 conversion has been performed as well. Although the results of the analysis were qualitative in nature, the same trends as for the tungsten compounds have been observed.

The kinetics of the tungsten oxide reduction/sulfidization process was inferred from XRD measurements, and some typical results are presented in Table 2. From this table it is clear that, in addition to the experimental parameters, the size of the oxide particles plays an important role in the reduction/sulfidization reaction. For large (3–5 μm) particles, the reduction to the suboxide $\text{W}_{20}\text{O}_{58}$ and the subsequent sulfidization into WS_2

occur between 570 and 650 $^\circ\text{C}$, whereas a powder consisting of small (0.1 μm) trioxide particles reacts at 400 $^\circ\text{C}$. Furthermore, whereas the sulfidization of small particles occurs in a mode which leads to fullerene formation, the large particles form turbostratic-like WS_2 particles at temperatures lower than 600 $^\circ\text{C}$, and 2H- WS_2 platelets upon sulfidization at elevated temperatures. In the absence of H_2S in the reactor, the reduction process is incomplete, and hence, it can be concluded that this gas serves as an auxiliary reducer of the oxide. Finally, the lower the concentration of hydrogen in the forming gas mixture, the slower was the reaction and the higher was the temperature required for the reaction. These considerations permit one to fine-tune the reaction conditions to the point that the IF- MS_2 phase can be synthesized with a very good reproducibility and yield.

Having the details of the reaction mechanism in mind, a modified reactor for the synthesis of macroscopic quantities of IF- WS_2 was constructed. The cross section of this reactor is illustrated schematically in Figure 5. To increase the amount of the (oxide) reactant and expose its entire surface to the gas, a bundle of tubes 7 mm in diameter each was placed inside the main tube (40 mm diameter) and the oxide powder was dispersed in them, very loosely. Typically, 1 g of IF- WS_2 could be obtained in a single batch, with a conversion yield of almost 100%.³⁰ This is remarkable in so far as the yield of production of carbon-nested fullerenes (and nanotubes) by the arc-discharge method is a few percent only.

In postulating a likely mechanism, we bear in mind the following: First, the reduction by H_2 is fast; the lower oxide is formed. Second, the formation of a thin sulfide skin controls the size of the fullerene. Since the size is thus fixed, the further transformation to sulfide must then take place internally.

A radial diffusion inward of the reactant (H_2S) and a similar diffusion outward of the product (H_2O) through the nanoparticle walls would appear unlikely in this case. Also, the large differences in time scales for the oxide reduction and the

(27) Reference 26, p 135.

(28) Sheng, E.; Sutherland, I. *Surf. Sci.* 1994, 314, 325.

(29) Reference 26, p 207.

(30) The major loss occurred from the evaporation of the oxide prior to the conversion with the first layer of the sulfide.

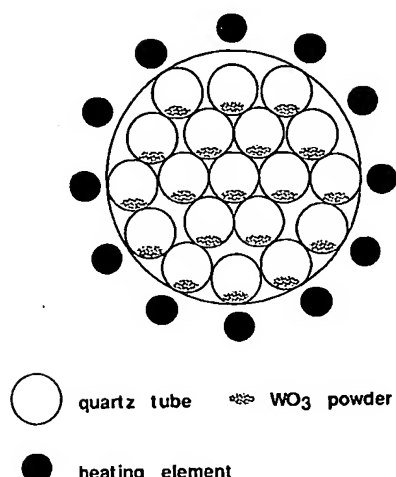


Figure 5. Cross section of the reactor which was used for the synthesis of bulk quantities of IF-WS₂.

subsequent sulfidization reaction suggest a different mechanism for the diffusion of hydrogen–oxygen and sulfur. It is hypothesized that the hydrogen and oxygen may diffuse through the layers (IIc) radially, while sulfur atoms intercalate and diffuse easily along the MS₂ layers (Lc) until they reach a dislocation or other fault which permits them to diffuse radially through the layer (||c) to the next inner layer. Such a mechanism would explain the fact that a single growth front is seen to advance away from structural defects at corners of the polyhedra (Figure 2C). The lattice expansion of ca. 20% of the c-axis, at

the high temperature of the process (1100 K), facilitates the intercalation/diffusion of the reacting species.

Conclusions

Since the outer surface of the IF material exposes only the basal plane of the compound, this material lends itself to solid lubrication applications. Indeed, IF nanoparticles do not stick to each other or the substrate and exhibit poor surface adhesion. Their approximate spherosymmetric shapes imply easy sliding and rolling of the nanoparticles, and consequently very small shear forces are required to move them on the substrate surface. Preliminary results tend to support this hypothesis.³¹ The oxide core (Figure 2C) provides the necessary mechanical toughness to the IF particle. Preliminary experiments indicate poor catalytic activity of the material, which is understandable, considering the surface termination by inert sulfur atoms. On the other hand, the potential of IF material for photocatalysis is promising due to the strong optical absorption, large surface area, and documented chemical inertness under illumination.³²

Acknowledgment. This research was supported by the following agencies: US-Israel Binational Science Foundation, Petroleum Research Fund of the American Chemical Society, NEDO (Japan), Edith Reich Foundation of the Weizmann Institute, UK-Israel S&T Research Fund, and Israeli Ministry of Energy and Infrastructure (R&D branch).

JA9602408

(31) Rappoport, L.; Feldman, Y.; Homyonfer, M.; Cohen, S.; Tenne, R. To be published.

(32) Tributsch, H. *Structure and Bonding*; Springer Verlag: Berlin, 1982, Vol. 49, p 127.



**OFFICIAL BUSINESS
PENALTY FOR PRIVATE USE, \$300**

AN EQUAL OPPORTUNITY EMPLOYER

United States Patent and Trademark Office
P.O. Box 1450
Alexandria, VA 22313-1450
If Undeliverable Return in Ten Days

RECEIVED
OCT 03 2006
USPTO MAIL CENTER

MART522* 852822119 1906 38 09/29/06
MARTINEZ' GREG RETURN TO SENDER
MOVED LEFT NO ADDRESS
UNABLE TO FORWARD
RETURN TO SENDER

卷之三

**This Page is Inserted by IFW Indexing and Scanning
Operations and is not part of the Official Record**

BEST AVAILABLE IMAGES

Defective images within this document are accurate representations of the original documents submitted by the applicant.

Defects in the images include but are not limited to the items checked:

- BLACK BORDERS**
- IMAGE CUT OFF AT TOP, BOTTOM OR SIDES**
- FADING TEXT OR DRAWING**
- BLURRED OR ILLEGIBLE TEXT OR DRAWING**
- SKEWED/SLANTED IMAGES**
- COLOR OR BLACK AND WHITE PHOTOGRAPHS**
- GRAY SCALE DOCUMENTS**
- LINES OR MARKS ON ORIGINAL DOCUMENT**
- REFERENCE(S) OR EXHIBIT(S) SUBMITTED ARE POOR QUALITY**
- OTHER:** _____

IMAGES ARE BEST AVAILABLE COPY.

As rescanning these documents will not correct the image problems checked, please do not report these problems to the IFW Image Problem Mailbox.